Energetic factors governing injection, regeneration and recombination in dye solar cells with phthalocyanine sensitizers†

Eva M. Barea,[a] Javier Ortiz,[b] Federico J. Payá,[b] Fernando Fernández-Lázaro,[b] Francisco Fabregat-Santiago,*[a] Angela Sastre-Santos*[b] and Juan Bisquert*[a]

Received 24th June 2010, Accepted 6th August 2010
DOI: 10.1039/c0ee00185f

Phthalocyanines (Pcs) are promising candidates for photon collectors for the near-infrared region of the solar spectrum in dye solar cells (DSC). Using two new Pc sensitizers, differing only in their Zn or metal-free center, we discuss the behaviour of the Pc dyes as sensitizers in DSC, and their influence on the solar cell performance, in comparison with standard N719 dye, at identical electrolyte conditions. Based on the separate identification of recombination resistance and the energy levels of titania by impedance spectroscopy, we determine the recombination rates and we also map the energies of the relevant components of the solar cells. An integration of the absorbance of the three sensitizers with the solar spectral distribution shows that electron injection should be similar for all the dyes (although 20% less in the case of the Pc with Zn center). However, since the LUMO level of these Pcs is low on the energy scale, it is necessary to use an electrolyte that keeps the conduction band of titania down to obtain some injection from the Pcs. Hence, the photovoltage is limited because the conduction band of titania is at a much lower position than in normal DSCs. We find that the conduction band of titania with the metal-free Pc is located on a similar energy level as for N719, and the recombination rate is not significantly different from the N719 cell. The main reason for the lower performance of this Pc is the lower injection than the ruthenium complex. In the case of the ZnPc, the conduction band is at higher energy than for N719. This allows that the V_{oc} obtained in these two samples becomes nearly the same despite the lower electron injection in the Zn phthalocyanines.

Introduction

Dye-sensitized solar cells (DSC) have attracted significant interest as a low-cost alternative to conventional silicon solar cells.[1,2] Usually, DSCs consist of a dyed nanoporous TiO_2 photoelectrode and a platinized counter electrode, filled with an organic electrolyte comprising I^-/I_3^- redox couple as the hole transport material (HTM). One of the key components for obtaining high power conversion efficiencies is the dye sensitizer, which should harvest light matching the solar spectrum. At present, the most successful charge-transfer sensitizers employed for these cells are polypyridylruthenium complexes, which yield solar-to-electric power conversion efficiencies of up to 11.3% at 1 sun (= 100 mWcm^2 1.5 air mass global).[3] However, Ru-complexes exhibit limited light-harvesting capabilities, particularly for the near-infrared region.[4,5] Consequently, many research efforts have been focused to collect the energy from this part of the solar spectrum, with phthalocyanines (Pcs)[6,7] being promising candidates due to their strong Q band light absorption properties at around 700 nm. Their extreme stability against thermal, chemical, and photochemical reactions is a definitively advantageous feature for the long-term and outdoor robustness of DSC.[8] In addition, it has recently been shown that Pc dyes in DSCs can be excited not only by red photons, but also by excitons *via* Förster resonant energy transfer (FRET).[9,10]

Although Pcs, and more generally organic dyes ZnPc, are good candidates for DSC sensitization,[11,12] at present, cells

[a]*Grup de Dispositius Fotovoltaics i Optoelectrònics, Departament de Física, Universitat Jaume I, 12071 Castelló, Spain. E-mail: bisquert@fca.uji.es*
[b]*División de Química Orgánica, Instituto de Bioingeniería, Universidad Miguel Hernández, 03202 Elche, Spain*

† Electronic supplementary information (ESI) available: Materials, characterization techniques, and experimental protocols; determination of energy levels; recombination and series resistance. See DOI: 10.1039/c0ee00185f

Broader context

While dye-sensitized solar cells (DSC) experience intense progress and development, harvesting light in the red part of the solar spectrum, where standard Ru-based sensitizers absorption is weak, remains a major issue. Here we explore the operation of DSC with phthalocyanine as sensitizers. These molecular dyes present strong absorption properties at around 700 nm, and extreme stability against thermal, chemical, and photochemical reactions. With analysis of impedance spectroscopy and steady state performance at 1 sun illumination intensity, we show that the performance of these sensitizers could be comparable to standard N719 dye, in terms of kinetic properties. However an energy diagram shows that the excited state of the phthalocyanines is very low, which limits the injection to TiO_2 and also the photovoltage obtained in the DSC.

incorporating Pcs as sensitizers show low efficiencies mainly due to (a) the low values of the open circuit potential (V_{oc}), and short-circuit current (j_{sc}), which affect the overall photon to electron conversion, and (b) the problems associated with the aggregation of Pcs on the metal oxide surface, that produces rapid deactivation of the dye excited state and low sensitizing efficiency. To investigate in detail the performance of new Pc sensitizers, we present here a study of the energetic and kinetic factors of Pc-sensitized DSC in comparison with DSC sensitized with the standard polypyridylruthenium N719 dye.

The operation of a high performance DSC requires fine tuning of a wide number of aspects that provide an optimal operation of different elements. In principle, in any solar cell of a single bandgap material the efficiency limit is set by two factors: (1) absorption of all photons with energy larger than the bandgap and subsequent charge separation, and (2) radiative recombination in the absorber. These factors establish the well-known Schockley-Queisser (SQ) limit.[13,14] In the scheme of Fig. 1 we can appreciate the absorption of light by the absorber (the dye in a DSC). According to SQ, the photovoltage should be determined by the width of the gap less a reduction by the radiative recombination. In addition, recombination at the maximum power point determines the fill factor (FF).

However, in a DSC there are additional important aspects to consider. The absorber material is connected from outside by two additional materials, the electron carrier (TiO_2) and the HTM. An effective electron-hole separation requires a price in the energetic arrangement of the materials to facilitate both the electron injection into the TiO_2 conduction band, and the regeneration of the oxidized dye by hole transference to the HTM. The open-circuit voltage is set by the maximum separation between the Fermi level of electrons in TiO_2 (E_{Fn}) and the Fermi level (electrochemical potential) of the holes/ions in HTM (E_{Fp}), under illumination. Clearly, the energy differences for injection and regeneration produce a significant reduction of the open-circuit voltage, as indicated in Fig. 1, with respect to SQ approach. It should be emphasized that such energy differences can be reduced, for example it is possible to shift upwards the conduction band of TiO_2 by appropriate absorbants in the electrolyte.[15,16] However this will usually have the effect of the dye injecting less efficiently into the TiO_2, with a loss in photocurrent. Therefore, the margin of efficiency increase by such manipulations is set by the intrinsic properties of the dye and the HTM.[17]

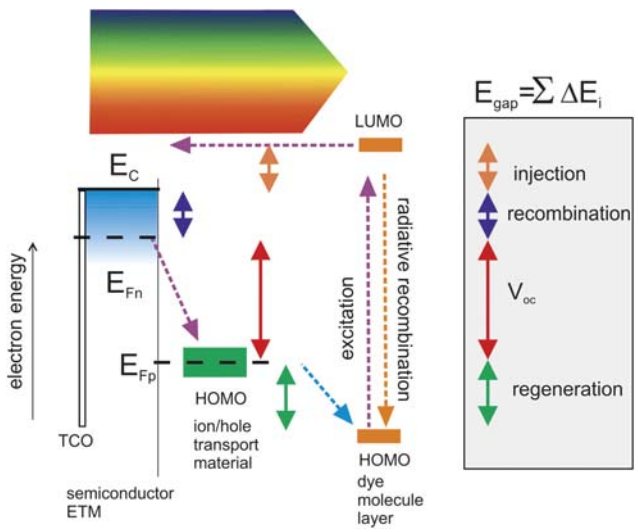

Fig. 1 Sketch of the energy diagram showing light absorption and charge transfer processes that occur in the dye solar cell at an open circuit. The origin of each of the energy losses in the solar cell associated with injection, recombination and dye regeneration is indicated, showing how the maximum potential theoretically attainable by the solar cell, the gap energy of the dye, E_{gap}, is reduced to the actual open-circuit voltage V_{oc}. For the sake of presentation clarity, the dye is not represented at the interface of the electron and hole transport materials, but separately on the right. E_C represents the conduction band edge, E_{Fn} the electron Fermi level, E_{Fp} the hole Fermi level, and TCO the transparent conducting oxide acting as electron collector. Dashed arrows indicate the direction of the electron flow in the mentioned processes, while the plain arrows indicate the energy difference.

The other aspect, which is crucial for solar cell operation, is the mechanism of recombination. As mentioned, in the SQ model, this is established by the reciprocal of light absorption, which is light emission from the absorber (*i.e.*, radiative recombination).[14] However, in a DSC the extent to which radiative recombination occurs in the dye itself is minor.[18] In fact, in a DSC electron and hole transport materials are spatially close to each other in the nanostructured configuration, and recombination is a charge transfer process between such media. Given that charge transfer in a DSC is controlled by the electronic events at the surface of titania nanoparticles, the recombination mechanism implies nonidealities with respect to SQ model that reduce the fill factor.[19]

It is usually said that the upper limit to the rise of the electron Fermi level in a DSC is the position of the conduction band of titania, E_C. This is a point with a high density of electronic states in the semiconductor, and certainly E_{Fn} cannot rise higher than this. However, as a matter of fact E_{Fn} is limited by recombination, as already mentioned. To our knowledge, a quantification of the distance between E_{Fn} and E_C at 1 sun has not generally been discussed. This is one of the aims of the present work. It should be important to quantify whether the present configurations of DSC admit significant room of improvement for V_{oc} by reduction of recombination.

In this paper, we study the behavior of DSCs sensitized with a new zinc phthalocyanine (ZnPc-1) and its free base counterpart (H_2Pc-2), Fig. 2, and refer the results to the scheme of Fig. 1. We used a cell with the commercial sensitizer N719 as reference. We have addressed the problem of charge injection, recombination and accumulation with the different dyes, in identical electrolyte conditions, using impedance spectroscopy (IS). This technique has been widely established as a central tool for detailed characterization of DSCs.[20,21] It allows separating the electrical contributions from the different elements composing the solar cell and discriminates their influence in the overall response of the device. An important advantage of IS with respect to other approaches is that the capacitance and recombination resistance are measured simultaneously. We are thus able to form quantitative energy diagrams and to discuss the performance of the given DSCs in relation to injection, energetics and recombination.

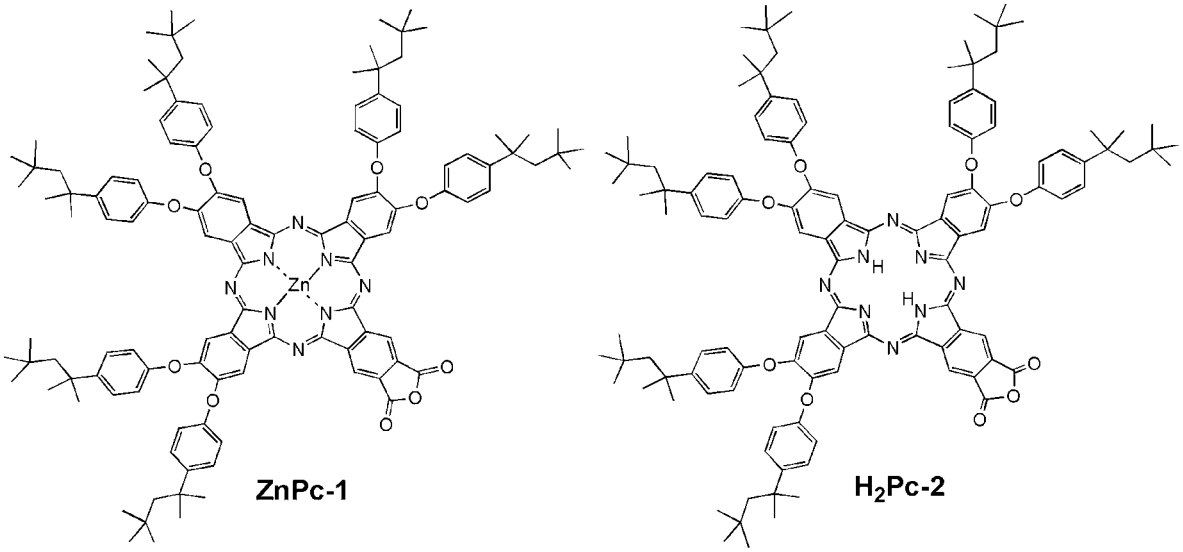

Fig. 2 Structures of the ZnPc-1 and H_2Pc-2 phthalocyanines used in this study.

The results indicate that the recombination flux in DSCs with the studied Pc dyes is not substantially higher than with standard N719 dye, and the lower injection is the reason why the performance of these Pc-based DSCs is inferior. The small energetic difference between the LUMO (lowest unoccupied molecular orbital) of the dye and the conduction band edge in TiO_2 seems to be responsible for this poor injection. The presence or absence of a metal center in the Pc changes the interaction of the dye with the TiO_2 surface, modifying the solar cell performance by modulation of the position of the titania conduction band.

Experimental

Solar cell manufacturing was carried out by Doctor-Blading TiO_2 layers on Transparent Conducting Glass - TCO glass (Pilkington TEC15, ~15Ω/sq resistance). Previously, a compact layer of TiO_2 (~100 nm) was deposited by spray pyrolysis in order to avoid the possible electron/electrolyte recombination reaction at the SnO_2 surface.[22] The produced transparent photoelectrodes of 8 μm thickness were sintered at 450 °C and then immersed into a 0.04 M $TiCl_4$ solution for 30 min at 70 °C followed by calcination at 450 °C for 30 min. When the temperature decreased down to 40 °C, the electrodes were immersed into the dye solution (0.3 mM in chloroform) for 4 h. After the adsorption of the dye took place, the electrodes were rinsed with pure chloroform.

The solar cells were assembled with a thermally platinized TCO counter electrode using a thermoplastic frame (Surlyn, Dupont 50 μm thick). The redox electrolyte (as detailed below) was introduced through a pre-drilled hole at the counter electrode, which was sealed afterwards. The assembled solar cells (with surface 0.35 cm^2) were characterized by current density–voltage (*j–V*) characteristics and IS. The photocurrent and voltage were measured using a solar simulator equipped with a 1000W ozone-free Xenon lamp and AM 1.5 Global filter (Oriel), using a 0.25 cm^2 mask. The light intensity was adjusted with an NREL-calibrated Si solar cell with a KG-5 filter to 1 sunlight intensity (100 $mWcm^{-2}$).

Results and discussion

Sensitizers

The new ZnPc-1 and H_2Pc-2 dyes have been designed taking into account the well-known directives described in the literature for their use in DSCs[22,23] in order to avoid aggregation phenomena, low solubility and lack of directionality in the excited state. One of the essential requirements for the light-harvesting system of a molecular/semiconductor junction is that the sensitizer possesses directionality of its electronic orbitals in the excited state. This directionality should be arranged to provide an efficient electron transfer from the excited state of the dye to the TiO_2 conduction band by good electronic coupling between the lowest unoccupied molecular orbital (LUMO) of the dye and the Ti 3d orbitals.[24] The Pcs used in this study bear sterical hindering *tert*-octylphenoxy groups to minimize the π–π stacking aggregation and to enhance solubility, as well as the electron releasing ability (push). They also contain an anhydride group, not only to facilitate anchoring to the nanocrystalline titanium dioxide semiconductor but also to act as electron withdrawing (pull) groups.

Therefore, the synthesis of the Pcs used in this study was carried out following the procedure indicated in the ESI (Fig. S1).† In a first step, the dicyanosubstituted Pc was obtained by statistical condensation of the 5,6-bis[4′-(1″,1″,3″,3″-tetramethylbutyl)phenoxy]-1,3-diiminoisoindoline with the 5,6-dicyano-1,3-diiminoisoindoline in 17% yield. Hydrolysis of the corresponding dicyanosubstituted Pc followed by dehydration of the dicarboxylic acid using acetyl chloride afforded the desired H_2Pc-2 (**2**). Finally, ZnPc-1 was prepared by metalation ($ZnCl_2$, DMAE/ODCB) of the free base H_2Pc-2. All compounds were fully characterized using the standard spectroscopic and analytical techniques, giving satisfactory results. In particular, the structures of both Pcs were assessed by MALDI-TOF mass spectrometry, ^{1}H-NMR, UV/vis, and IR spectroscopy (see ESI, Fig. S2–S5).† The ^{1}H NMR spectrum of H_2Pc-2 in $CDCl_3$ shows four broad singlets integrating for two protons, each

corresponding to the phthalocyanine ring at 8.60, 8.39, 8.31 and 8.08 ppm, due to the C_{2v} symmetry of the molecule. Two groups of doublets for the *meta* and *orto* hydrogens of the phenoxy groups between 7.53 and 7.16 ppm and three sets of singlets for the tetramethylbutyl substituents: 1.77, 1.78 and 1.85 for six methylene units; 1.48 and 1.40 for twelve methyl groups and 0.90, 0.80 and 0.75 for six *tert*-butyl groups, were also observed. Finally at −3.25 ppm a broad singlet appears due to the two NH hydrogens of the phthalocyanine. A similar spectrum was obtained for ZnPc-1 using THF-d_8 as solvent instead of $CDCl_3$ to avoid aggregation, except for the signal of the two NH which disappears.

The electronic absorption spectra of the two Pcs were recorded in chloroform solution and compared with those of the Pcs adsorbed onto transparent nanocrystalline TiO_2 films, Fig. 3. The absorption spectrum in solution consists of a Soret band at 356 and 363 nm for H_2Pc-2 and ZnPc-1, respectively. Additionally, two Q-bands centered at 673 and 703 nm for H_2Pc-2 and one Q-band at 682 nm for ZnPc-1 due to π–π* transitions of the conjugated macrocycle are observed. When the molecules are adsorbed on TiO_2, the absorption peaks broaden, but show no shift in the peak position compared to the dyes in solution, which suggests negligible or minor aggregation of the attached dye. We remark that the time of absorption of all dyes is just four hours. As a further test, 3 mM chenodeoxycholic acid, which is known to prevent the dye aggregation on the TiO_2 surface, was added to the dye sensitizing solution. The UV-Vis spectra of these new samples (not shown) match exactly the spectra shown in Fig. 3(a) and 3(b) for sensitizers absorbed on a nanocrystalline transparent TiO_2 film (dashed line). Additionally, the same current–voltage characteristics were obtained.

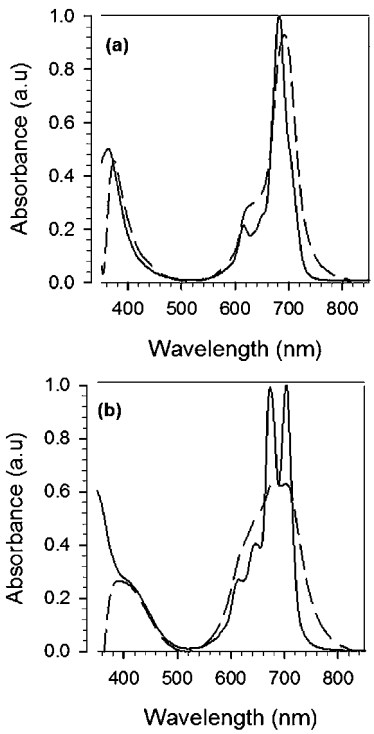

Fig. 3 UV-vis absorption spectra of ZnPc-1 (a) and H_2Pc-2 (b) in chloroform (solid line) and adsorbed on a nanocrystalline transparent TiO_2 film of ~8 μm thickness (dashed line).

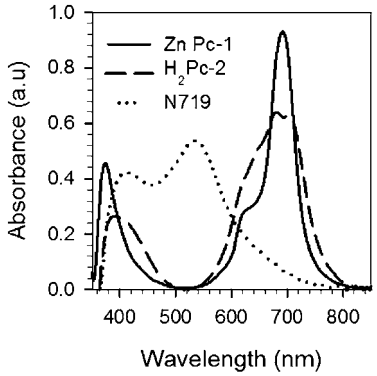

Fig. 4 UV–vis spectra of ZnPc-1, H_2Pc-2 and N719 adsorbed on a nanocrystalline transparent TiO_2 film.

Fig. 4 compares the absorption of ZnPc-1 and H_2Pc-2 dyes with N719 as reference. It may be mentioned here that the absorption spectra of the Pcs are complementary to those of N719, which makes them suitable for fabricating tandem or cocktail solar cells.

Solar cell study

Fig. 5(a) compares the *j–V* curves for DSCs sensitized with ZnPc-1, H_2Pc-2 and N719 as reference. To ensure the reproducibility and consistency of the results, the experiments were repeated 3 times, building fresh solar cells each time, and determining *j–V* curves and IS data for all the samples. Furthermore, the cells were measured prior to and after the impedance measurements. No significant changes were observed out of those related to sample heating after 8 h at 1 sun illumination. Therefore, the results presented below are highly representative of the behaviour of the dyes used.

Cyclic voltammetry measurements of the Pcs in solution indicated LUMO levels in these dyes are at lower potential than in the case of N719 (Table S1 in the ESI).† Therefore no further additives such as 4-*tert*-butylpyridine or *N*-methylbenzimidazole, which are known to rise the conduction band edge of the TiO_2 (E_C), were added to the electrolyte and a high concentration of Li^+ was used, instead of, for instance, guanidinium thiocyanate, to keep the E_C at sufficiently low values[25] to be able to inject efficiently the electrons from the excited Pc dyes. In order to compare the results among these dyes and N719, all solar cells were made with the same electrolyte: 0.7 M LiI (99.9%) and 0.05M I_2 (99.9%) in 3-methoxypropionitrile. Obviously, the performance of the sample with the N719 dye in this configuration is far from optimal. The details of an optimized cell with N719 are given in the ESI.† With modified electrolyte to raise up the conduction band and 14 h absorption time the normal DSC with N719 provides a conversion efficiency of 7.20% at 1 sun, see Fig. S6.†

Overall, the results in Fig. 5(a) and Table 1 show that for all cells, the values of V_{oc} for N719 and ZnPc-1 samples are similar, being somewhat higher for N719. However, in the case of H_2Pc-2, V_{oc} is 90 mV lower. The main difference between the dyes is the photocurrent. To understand the causes of the different performances, we made IS measurements under 1 sun illumination of all the prepared DSCs, sensitized with the different dyes: ZnPc-1,

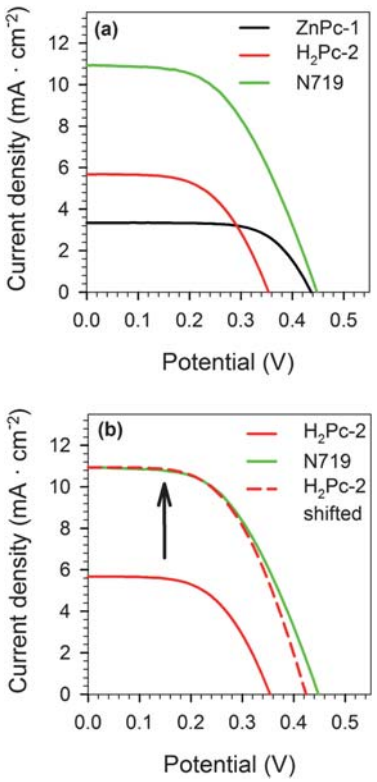

Fig. 5 (a) Current density-potential curves for DSCs with ZnPc-1, H_2Pc-2 and commercial N719 as sensitizers, at 1 sun light intensity. (b) The continuous lines represent *j–V* curves of H_2Pc-2 and N719 as in (a), while the dotted line plots the *j–V* curve of H_2Pc-2 shifted upwards until j_{SC} matches that of N719.

Table 1 Photovoltaic performance parameters and the estimated position of the conduction band of DSCs using ZnPc-1, H_2Pc-2 and N719 as sensitizers. j_{SC} is the short circuit photocurrent density, V_{oc} the open-circuit voltage, *FF* the fill factor, η the power conversion efficiency, *n* the electron density at open circuit potential, E_C the energy *vs.* vacuum of the conduction band edge position and E_{Fn} the Fermi level of electrons in the TiO_2 at open circuit conditions

Sample	V_{oc}/ V	j_{sc}/ mA cm^{-2}	*FF*	η (%)	*n* at V_{oc}/ cm^{-3}	E_C/ eV	$E_C - E_{Fn}$/ eV
ZnPc-1	0.44	3.48	0.66	1.01	4.2×10^{17}	−4.00	0.31
H_2Pc-2	0.35	5.71	0.57	1.14	1.5×10^{18}	−4.13	0.27
N719	0.45	10.90	0.51	2.50	3.0×10^{18}	−4.11	0.19

H_2Pc-2 and N719. The main parameters obtained from IS measurements are shown in Fig. 6.

For analyzing the parameters resulting from IS data treatment, it is essential to plot the results on the adequate potential scale. The measured potential needs to be corrected from series resistance, R_{series}, losses in the cells, which provides a potential drop not associated with the displacement of the Fermi level. In general, there are several contributions to R_{series}: the sheet resistance of FTO glass collector, R_{FTO}, the charge transfer resistance at the platinized counter-electrode in the electrolyte regeneration process, R_{Pt}, the electron transport resistance in the TiO_2 matrix, R_{tn} and the diffusion resistance of the holes in the electrolyte, R_D. The total series resistance of the cell is

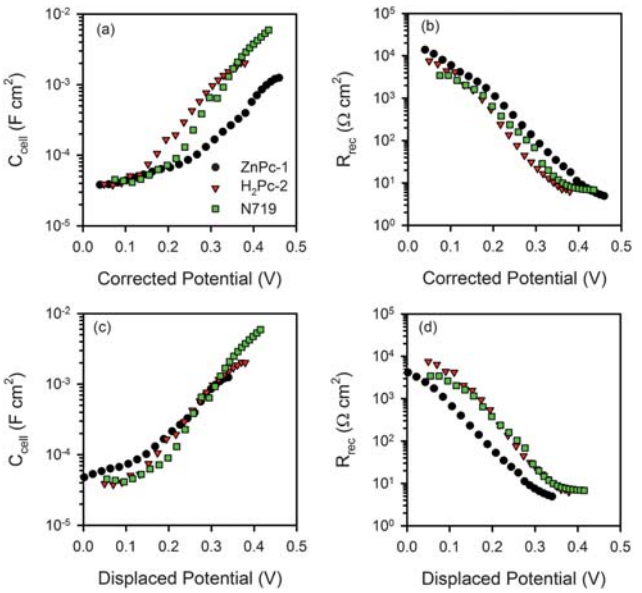

Fig. 6 Capacitance (a) and recombination resistance (b) obtained from impedance spectroscopy of the solar cells with ZnPc-1, H_2Pc-2, and commercial N719 as sensitizers under illumination. The potential is corrected from a series resistance drop. In (c) and (d) the capacitance and recombination resistance are displaced, by the amounts −20 mV in the case N719 and −130 mV ZnPc-1, to make all capacitances overlap and ensure the same electron concentration in TiO_2. In these conditions R_{rec} of N719 and H_2Pc-2 superimpose each other while ZnPc-1 presents smaller values.

$R_{series} = R_{FTO} + R_{Pt} + R_{tn}/3 + R_D$. In this case, R_{FTO} and R_{Pt} were similar in all samples, while both transport and diffusion resistances had negligible values at 100 mW cm^{-2}. Therefore the total R_{series} yielded values ranging between 15 and 30 Ω.

The measured capacitances of the cells are shown in Fig. 6(a). The dominant capacitances of DSC in the low potential region are given by the back layer capacitance and the interfacial capacitance at the platinized counter-electrode, which are nearly constant.[18] At higher potentials, the chemical capacitance of TiO_2, C_μ, governs the capacitive response of the cell. C_μ depends on the density of electronic states (DOS) in TiO_2, *g*(E), at the Fermi level of electrons (E_{Fn})[26] *via*

$$C_\mu = L(1 - p)\, q\, g(E_{Fn}) \quad (1)$$

where *L* represents the TiO_2 film thickness, *p* its porosity, and

$$g(E_{Fn}) = \frac{\alpha\, qN_L}{k_B T} \exp[\alpha(E_{Fn} - E_C)/k_B T]\,, \quad (2)$$

with N_L the total density of bandgap states, *q* the elementary charge, k_B the Boltzmann constant, and α the parameter that describes the exponential trap distribution of electrons below the conduction band.[26]

Since the capacitance corresponds to a chemical capacitance that shows the density of states in the bandgap of TiO_2,[26] the displacement of capacitance plots in Fig. 6(a) indicates the displacement of the conduction band in TiO_2 in the DSC. As film thickness and porosity is the same for all the samples, these data show that the conduction bands in H_2Pc-2 and N719 are shifted downwards with respect to its position in ZnPc-1. This effect may

be attributed to the presence of a proton excess in the H_2Pc-2 and N719 dyes that interacts with the TiO_2 surface and lowers the conduction band of the semiconductor, with respect to ZnPc-1.[27–31] Stable proton transfer complexes between H_2Pcs and amines have been observed in the literature.[32,33] In the case of N719, an additional contribution to this displacement could be attributed to the interaction between TiO_2 surface and the different dye structures.

Taking H_2Pc-2 as reference, the relative shift of the E_C in the TiO_2 may be easily estimated by displacing the chemical capacitances until they all match, as shown in Fig. 6(c). Proceeding in this way, ΔE_C is found to be 20 mV for N719 and 130 mV for ZnPc-1.

The slopes of C_μ for H_2Pc-2 and ZnPc-1 samples are nearly the same, while that of N719 is slightly higher, indicating that the interaction of N719 with the TiO_2 surface modifies the trap distribution density. It may be observed that the capacitance of the TiO_2 in H_2Pc-2 and ZnPc-1 has a lower limit at the highest potentials than in the case of N719. This limitation is attributed to the presence of a low frequency inductive behavior (negative capacitance)[34,35] in both Pc samples at these voltages, which is not present in the case of the N719 sample. Negative capacitance is related to a charge transfer process between two electronic reservoirs that is governed by the occupation of an intermediate state, which becomes saturated and limits the kinetics of the process.[36] In a recent paper, this intermediate state has been associated with the presence of surface states at the TiO_2.[37] In our case, the data obtained suggest that the differences between the Pcs and the N719 in the number and distribution of these surface states are small and not enough to modify R_{rec}.

The energy diagram

To build a practical representation of the scheme presented in Fig. 1, which quantitatively describes the energetics of the DSC with the three sensitizers, we need to set the specific energy levels of the different elements used in the DSCs. In Fig. 7 the energetics of the titania (which is crucial for determining recombination) is placed in the context of the other elements of the DSC. The diagram is constructed as follows.

The DOS of TiO_2, in each cell is plotted in Fig. 7 directly from the chemical capacitance (dots), while the lines are traced using eqns (1) and (2), which describe the trap distribution below the conduction band. In addition, using a value of the total number of trap states $N_L = 2 \times 10^{20}\,cm^{-3}$, it is possible to estimate the value of the energy of the conduction band edge as an extrapolation of the measured DOS. The value obtained for the different samples is presented in Table 1 and indicated with horizontal blue lines in Fig. 7. The actual rise of the Fermi level in the bandgap at 1 sun is indicated by the arrow that marks the extent of V_{oc}.

With these data it is possible to estimate the energy difference between the Fermi level at 1 sun and the conduction band. In these conditions, it is also possible to calculate the density of electrons in the TiO_2 that form the integration of the capacitance yields to

$$n(V_{OC}) = \frac{k_B T}{\alpha q^2} \frac{1}{L(1-p)} C(V_{OC}) \qquad (3)$$

Both sets of data are presented in Table 1.

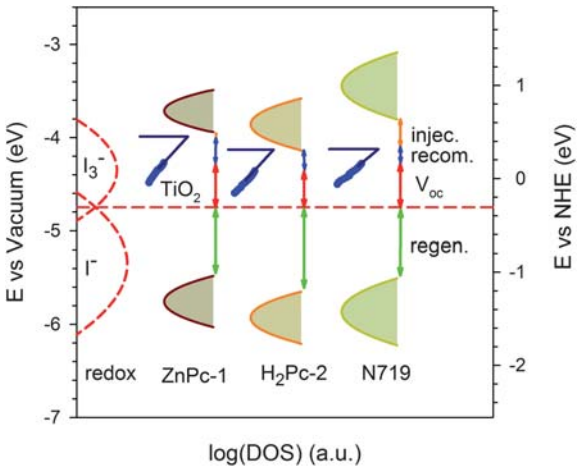

Fig. 7 Energy diagram of the active components in the DSC with the different dyes. Acceptor and donor states of the I_3^-/I^- redox couple (dashed line), taking reorganization energy of 0.5 eV; HOMO and LUMO states of the dyes after considering absorption and solvation effects (continuous lines); density of electron states below the conduction band of the TiO_2, obtained from capacitance measurements (dots) and estimated shape up to the conduction band (blue line). The dotted line represents the TiO_2 density of states with optimised electrolyte.

To represent the energy levels of the redox couple, we used a normal distribution to describe the fluctuating acceptor and donor states of the I_3^-/I^- redox couple (dashed line), taking as solvent reorganization energy 0.5 eV as estimated by Miyashita *et al.*[38] and standard redox energy of 0.35 eV *vs.* NHE.[39] The lower intensity of I_3^- is related to the lower concentration of this species. This distribution is a simplification of the measured one by Cao *et al.*,[40] to facilitate the interpretation of data.

The HOMO (highest occupied molecular orbital) and LUMO states of the dyes have also been represented in Fig. 7 using normal distributions. This approximation allows to include energy dispersion effects such as the vibronic levels of the dye, solvation by electrolyte, and energy dispersion due to adsorption of the dye at different TiO_2 sites. Again for the purposes of simplicity, the complete distribution of states in the acceptor (unoccupied) and donor (occupied) molecular orbitals is not represented here. The top energy position of the HOMO has been determined by cyclic voltammetry (see Table S1 in the ESI)† for the phthalocyanines and it has been taken from the literature for the N719.[3,41] The energy position of the bottom of the LUMO is determined by adding to the HOMO the energy of the gap calculated from the onset of the absorption in Fig. 4 (see more details in the ESI).† The width and height of the distribution of states has been taken to approximate the absorption spectra of Fig. 4.

Analysis of the solar cells performance

Using Fig. 7 as reference we now discuss the results obtained for the different dyes according to the photophysical mechanisms pointed out in Fig. 1.

Regeneration. It is depicted in Fig. 7 that the largest loss of potential in the DSC has its origin in the mismatch between the

HOMO of the dye and the Redox couple, as is well known in the literature.[39]

Injection. Incident current to photon efficiency (IPCE) measurements of Fig. 8, revealed the difference in the efficiency for charge injection of the different dyes. Integration of the IPCE's of ZnPc-1, H_2Pc-2 and N719 with a solar spectrum provided, respectively, 3.6, 6.4 and 12.4 mA cm^{-2}, that agree quite well with the short circuit photocurrent data observed for the samples, Table I.

It is a very relevant fact that LUMOs in phthalocyanines are at lower energies with respect to N719 and very close to the conduction band edge of TiO_2. As a consequence, the energy loss due to injection may be considered negligible. The drawback of the alignment of these levels is that the injection efficiency from the excited dye, D^*, to the semiconductor is expected to decrease,[42] especially after taking into consideration the fact that due to reorganization effects, the excited state D^* shifts downwards with respect to its position in the dye LUMO before absorbing the light. Therefore, it is necessary that the energy of the LUMO of the dye exceeds that of E_C in the TiO_2, to ensure an efficient electron injection from the dye. This is the case when using N719 instead of a Pc: If we compare the amount of light that may be absorbed by the H_2Pc-2 and the N719 by the integration of the absorption spectra of Fig. 4 with the solar spectrum, it provides the same result for the two dyes. Once discarded aggregation phenomena, the much smaller current found for the H_2Pc-2 indicates that this dye has a lower transfer rate of electrons from the excited dye to the TiO_2. Furthermore, we have confirmed that the injection can be suppressed completely with the introduction in the electrolyte of additives that rise TiO_2 conduction band edge.

Comparing now the light absorption efficiency of the H_2Pc-2 with respect to the ZnPc-1, using the data from Fig. 4, we can conclude that most of the decrease in the photocurrent observed has its origin in the lower number of photons absorbed by the ZnPc-1 which is 80% of the amount that the H_2Pc-2 does.

Other contributions to lower the injection efficiency in the Pc dyes could arise from a poor regeneration rate of the oxidized dye. We have not been able to carry out direct observation of the characteristic regeneration time of the dyes through transient absorption[43] or photoinduced absorption spectroscopy[44] experiments. An alternative way of evaluating dye regeneration is to measure the IPCE at different I^- concentration.[45] Therefore, we increased the concentration of I to 1M by adding to the previous electrolyte 0.2 M LiI and 0.1 M metylbenzimidazolium iodide (MBII). MBII was added to compensate an extra E_C downward shift given by the increased concentration of Li that would also produce an increase in the IPCE.

In the case of ZnPc-1 (Fig. 9(a)), the IPCE improved even though a slight upward shift in the conduction band of the TiO_2 was observed by means of impedance analysis (not shown). This indicates that the regeneration for this dye may be improved with an optimized electrolyte. In the case of H_2Pc-2, however, the IPCE drops down. In this case, we do not observe an improved regeneration, able to compensate the effect of the small band shift. These data suggest that while H_2Pc-2 regenerates at a similar rate as N719, ZnPc-1 regeneration is poorer. This may explain part of the other 14% loss in j_{SC} observed for the DSC made from ZnPc-1 with respect to H_2Pc-2.

Recombination and Fermi level equilibration. With the plot of Fig. 7 it is possible to evaluate the origin of the difference between charge transfer resistances in the different samples. According to the Marcus model, as applied in DSC,[46] the recombination takes place between levels at the same energy in

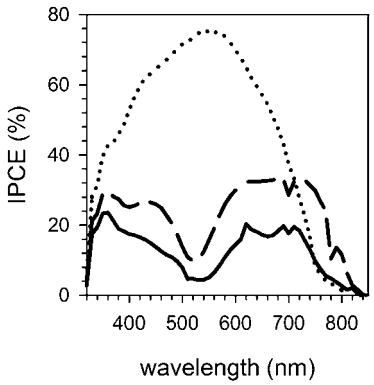

Fig. 8 IPCE of ZnPc-1 (line), H_2Pc-2 (dashed line) and N719 (dotted line) in complete solar cells using as electrolyte 0.7 M LiI and 0.05M I_2 in 3-methoxypropionitrile.

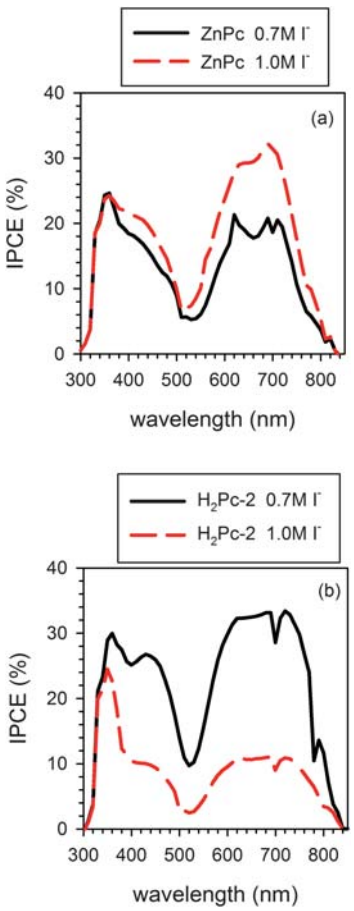

Fig. 9 IPCE of ZnPc-1 (a) and H_2Pc-2 (b) based DSCs with electrolytes containing 0.7 M and 1 M concentration of I^-.

TiO_2 and the redox acceptor. Therefore we can understand quantitatively that the higher the conduction band, the lower the recombination current, j_{rec}, at a certain potential due to the lower amount of electrons available to recombine.

Given that the recombination resistance, R_{rec}, is related to the recombination flux,[20,21]

$$R_{rec} = \left(\frac{\partial j_{rec}}{\partial V}\right)^{-1}, \quad (4)$$

the increase in E_C means a larger R_{rec}. This is the general result that can be observed in Fig. 6(b).

Data in Table 1 show that the large potential shift in the TiO_2 conduction band of the ZnPc-1 based DSC with respect to the H_2Pc-2 (110mV) is not fully reflected in the open circuit photopotential. As a consequence, the energy loss attributed to recombination (Fig. 7) is larger for the ZnPc-1. This fact is the result of the combination of two effects, both limiting the rise of the Fermi level in the TiO_2: the lower charge injection, just described above, and a larger relative recombination rate in the ZnPc-1, that we describe in more details in the following.

In the case of the H_2Pc-2 and N719 the values and slope of the capacitance, Fig. 6(a), and hence the distribution of the DOS below E_C are similar for both DSCs. They have also similar recombination resistances as shown in Fig. 6(b). When the data are corrected for the small observed band shift of the conduction band, Fig. 6(d), the match in R_{rec} is perfect, indicating that the recombination rate at the same electron concentration in the semiconductor, is the same for both dyes.

In the case of ZnPc-1, the larger value of R_{rec} shown in Fig. 6(b) provides the larger V_{oc} compared to H_2Pc-2. However, when the potential is displaced to compare all the results at the same electron concentration, Fig. 6(d), ZnPc-1 presents lower values than H_2Pc-2 and N719. This change in R_{rec} to values lower than 1/3 on average at the same electron density, may not be explained by a difference in the surface coating with the dye. The different matching between the acceptor states in the redox couple and the electron donor states in the TiO_2 with ZnPc-1 could be the main reasons of this variation. This suggestion agrees with a previous work by Peter and coworkers[27] where they showed that the variations of the lifetime measured with different dyes were due to the shift of the conduction band, and that differences in surface dipoles could be attributed to variation in the surface protonation.

In comparison with previous results, we should mention that the more efficient Pc named TT1, shows an efficiency of 3.52% with a short-circuit current of 7.60 $mAcm^{-2}$, and open-circuit voltage of 0.617 V.[12] We have not yet had the opportunity to study this dye. In another work by O'Regan *et al.*,[22] a number of Ru-Pcs is studied in comparison with N719 in identical electrolyte conditions. In this work it was first recognized that the conduction band of titania must be kept low, otherwise the Pcs do not inject. However, O'Regan *et al.*, attribute the lower performance of their Pcs, and the low voltage of organic dyes in general, to higher recombination. Our results presented above with the Pcs show that this is not the general case. We have shown that in a DSC with H_2Pc-2 the recombination rate is the same as in a DSC with N719 dye. The reason for the lower performance of H_2Pc-2 is clearly a lower injection, caused by the low position of the dye LUMO level, which is close to the conduction band of TiO_2. With increasing the injection (j_{SC}), V_{oc} increases as the distance E_C–E_{Fn} becomes smaller, Table 1.

Additional confirmation of this interpretation is obtained simply by displacing the j–V curve of H_2Pc-2 upwards, to simulate the *same* charge injection level (same j_{SC}) as that obtained in the case of N719. As can be seen in Fig. 5(b), very good agreement is found between both curves, indicating that at same injection level H_2Pc-2 would perform exactly the same as N719 (in these conditions of electrolyte). It should be noticed that this simple approach does not take into account other considerations such as the series resistance effect and the small difference in E_C (responsible for the 20 mV V_{oc} difference in the final curves).

In the Introduction, we commented on the interest to obtain quantitative determination of the distance between the electron Fermi level in titania, at 1 sun, and the edge of the conduction band. A preliminary answer to this question is given in Table 1. However, we must emphasize that the position of E_C is obtained by extrapolation of the measured DOS on the assumption that the total number of trap states is $N_L = 2 \times 10^{20}$ cm^{-3}. Unfortunately, the position of the conduction band in the energy scale is not yet unambiguously determined. Nonetheless these results indeed show potential for improvement, since E_{Fn} appears to lie far below the conduction band. The total electron density of electrons at 1 sun in open-circuit conditions, which is a *measured* quantity, provides values of the order of 10^{18} cm^{-3}. We believe that it should be possible to accumulate a far larger number of electrons in titania nanoparticles, by reducing recombination rates.

Summarizing, if recombination rates (R_{rec}) are similar, a high position of E_C provides a high value of V_{oc}. This value may be raised if the injection is increased, which reduces the distance E_C–E_{Fn}, increasing the electron concentration in the TiO_2 at open circuit potential, Table 1. The limits to this rise are the position of the E_C and the number of electrons injected from the dye that may be accumulated in the semiconductor in equilibrium, as established by recombination rates.

Fill factor. The last parameter to interpret from cell performance in Table 1 is the FF. The j–V curve generated by R_{rec} is modulated by the presence of a series resistance, R_{series}, that through the FF reduces the real performance of the solar cell.[20,21] Except for the case of N719-op (Fig. S6),† differences in the FF for the different samples shown in Table 1, are related to the increasing current passing through the cells. Indeed, the higher the current crossing the samples, the more important is the potential drop at R_{series}, yielding a smaller FF.[20,21]

From these results, we can state that the low performance of the DSC based on Pcs as dyes is not limited by higher recombination than N719, it is related to a limited photoinjection, due to mismatch of the conduction band of TiO_2 with the LUMO of the excited dye. These injection problems could be mitigated when the Pc presents additional acidic protons which gives rise both to a decrease of the TiO_2 E_C level[24] improving the injection, and also to the regeneration rate of the dye. Given that an electrolyte with a high concentration of Li is used, it doesn't seem feasible to bring further down the conduction band of titania in order to extract more current from these Pcs. Our study indicates that as

recombination is not the limiting factor in the efficiency of DSC, the major route to improve the Pc dyes is to shift up both their HOMO and LUMO levels on the absolute energy scale. The results given by the best DSCs based on Pc dyes point also in this direction.[12,47]

Conclusions

The phthalocyanine dyes H_2Pc-2 and ZnPc-1 have shown very good sensitization with high extinction coefficients in the 700 nm region which provides potential injection levels similar to N719 dye. Through capacitive measurements, TiO_2 conduction band position for the N719 and H_2Pc-2 sensitized cells has been found similar to and lower than in the case of the ZnPc-1, which has been attributed to the presence of protons in the first two dyes with respect to ZnPc-1.

The LUMO of the phthalocyanines has been found to be at lower levels than N719, limiting the injection from the dyes to the TiO_2. This places constraints on the electrolyte that can be used. The low position of the conduction band of titania imposes a low photovoltage. This, together with the limitations to injection, explains the relatively low performance of the Pc-based DSCs.

The main synthetic efforts about Pc sensitizers for DSC have been directed to designing a structure that avoids aggregation and provides the push–pull structure to facilitate electron injection. The low V_{OC} and photocurrent obtained have been usually attributed, respectively, to higher recombination and narrower gap than in DSCs with ruthenium polypyridyl complexes. Here we have found that both an inefficient injection and the low position of the conduction band of TiO_2, limited by the LUMO of the dye, are responsible for the achieved V_{OC}. Only in the case of ZnPc-1 (**1**) an improvement of the recombination resistance to values similar to that of N719 at the same electron concentration level would provide additional improvement in the photopotential. Future works will focus on both increasing the injection yield and raising up the energy levels of the Pc dye as critical factors for improving the performance of the solar cells made from these dyes.

In this paper it has been shown that the calculation of the Schokley-Queisser limit for the efficiency of dye solar cells needs to consider the different potential drops that reduce the potential energy from the gap of the absorber to the real V_{oc}. The greater of these potential losses is the mismatch between HOMO of the dye and the redox couple. The other potential drops due to injection and recombination may be manipulated to optimize the performance of the devices, although the intimate relation between those phenomena increases the difficulties to translate SQ calculations into real data.

Acknowledgements

We are grateful for financial support from Ministerio de Ciencia e Innovación under projects HOPE CSD2007-00007, MAT2007-62982 and CTQ2008-05901/BQU, and Generalitat Valenciana under projects PROMETEO/2009/058, ACOMP/2009/056 and ACOMP/2009/095.

References

1 B. C. O'Regan and M. Grätzel, *Nature*, 1991, **353**, 737.
2 J. Bisquert, D. Cahen, G. Hodes, S. Ruhle and A. Zaban, *J. Phys. Chem. B*, 2004, **108**, 8106.
3 M. K. Nazeeruddin, F. De Angelis, S. Fantacci, A. Selloni, G. Viscardi, P. Liska, S. Ito, B. Takeru and M. Grätzel, *J. Am. Chem. Soc.*, 2005, **127**, 16835.
4 Y. Shibano, T. Umeyama, Y. Matano and H. Imahori, *Org. Lett.*, 2007, **9**, 1971.
5 R. Neil, *Angew. Chem., Int. Ed.*, 2008, **47**, 1012.
6 P. Y. Reddy, L. Giribabu, C. Lyness, H. J. Snaith, C. Vijaykumar, M. Chandrasekharam, M. Lakshmikantam, J.-H. Yum, K. Kalyanasundaram, M. Grätzel and M. K. Nazeeruddin, *Angew. Chem., Int. Ed.*, 2007, **46**, 373.
7 G. de la Torre, C. G. Claessens and T. Torres, *Chem. Commun.*, 2007, 2000.
8 S. Eu, T. Katoh, T. Umeyama, Y. Matano and H. Imahori, *Dalton Trans.*, 2008, 5476.
9 B. E. Hardin, E. T. Hoke, P. B. Armstrong, J. H. Yum, P. Comte, T. Torres, J. M. Fréchet, M. K. Nazeeruddin, M. Grätzel and M. McGehee, *Nat. Photonics*, 2009, **3**, 406.
10 K. Shankar, X. Feng and C. A. Grimes, *ACS Nano*, 2009, **3**, 788.
11 J. He, G. Benkö, F. Korodi, T. Polívka, R. Lomoth, B. Åkermark, L. Sun, A. Hagfeldt and V. Sundström, *J. Am. Chem. Soc.*, 2002, **124**, 4922.
12 J.-J. Cid, J.-H. Yum, S.-R. Jang, M. K. Nazeeruddin, E. Martínez-Ferrero, E. Palomares, J. Ko, M. Grätzel and T. Torres, *Angew. Chem., Int. Ed.*, 2007, **46**, 8358.
13 W. Shockley and H. J. Queisser, *J. Appl. Phys.*, 1961, **32**, 510.
14 U. Rau, *Phys. Rev. B: Condens. Matter Mater. Phys.*, 2007, **76**, 085303.
15 Z. Zhang, S. M. Zakeeruddin, B. C. O'Regan, R. Humphry-Baker and M. Grätzel, *J. Phys. Chem. B*, 2005, **109**, 21818.
16 Z. Zhang, N. Evans, S. M. Zakeeruddin, R. Humphry-Baker and M. Grätzel, *J. Phys. Chem. C*, 2007, **111**, 398.
17 T. W. Hamman, R. A. Jensen, A. B. F. Martinson, H. V. Ryswykac and J. T. Hupp, *Energy Environ. Sci.*, 2008, **1**, 66.
18 T. Trupke, S. Naumgärtner and P. Würfel, *J. Phys. Chem. B*, 2000, **104**, 308.
19 J. Bisquert and I. Mora-Seró, *J. Phys. Chem. Lett.*, 2010, **1**, 450–456.
20 Q. Wang, S. Ito, M. Grätzel, F. Fabregat-Santiago, I. Mora-Seró, J. Bisquert, T. Bessho and H. Imai, *J. Phys. Chem. B*, 2006, **110**, 19406.
21 F. Fabregat-Santiago, J. Bisquert, E. Palomares, L. Otero, D. Kuang, S. M. Zakeeruddin and M. Grätzel, *J. Phys. Chem. C*, 2007, **111**, 6550.
22 B. C. O'Regan, I. Lopez-Duarte, M. V. Martinez-Diaz, A. Forneli, J. Albero, A. Morandeira, E. Palomares, T. Torres and J. R. Durrant, *J. Am. Chem. Soc.*, 2008, **130**, 2906.
23 M. K. Nazeeruddin, R. Humphry-Baker, M. Gratzel, D. Wöhrle, G. Schnurpfeil, G. Schneider, A. Hirth and N. Trombach, *J. Porphyrins Phthalocyanines*, 1999, **3**, 230.
24 L. Giribabu, C. V. Kumar, V. G. Reddy, P. Y. Reddy, C. S. Rao, S.-R. Jang, J.-H. Yum, M. K. Nazeeruddin and M. Grätzel, *Sol. Energy Mater. Sol. Cells*, 2007, **91**, 1611.
25 R. Caballero, E. M. Barea, F. Fabregat-Santiago, P. de la Cruz, L. Márquez, F. Langa and J. Bisquert, *J. Phys. Chem. C*, 2008, **112**, 14919.
26 J. Bisquert, *Phys. Chem. Chem. Phys.*, 2003, **5**, 5360.
27 W. H. Howie, F. Claeyssens, H. Miura and L. M. Peter, *J. Am. Chem. Soc.*, 2008, **130**, 1367.
28 M. K. Nazeeruddin, R. Humphry-Baker, P. Liska and M. Gratzel, *J. Phys. Chem. B*, 2003, **107**, 8981.
29 Y. Liu, A. Hagfeldt, X.-R. Xiao and S.-E. Lindquist, *Sol. Energy Mater. Sol. Cells*, 1998, **55**, 267.
30 F. Fabregat-Santiago, J. Bisquert, G. Garcia-Belmonte, G. Boschloo and A. Hagfeldt, *Sol. Energy Mater. Sol. Cells*, 2005, **87**, 117.
31 J. Bisquert, F. Fabregat-Santiago, I. Mora-Seró, G. Garcia-Belmonte, E. M. Barea and E. Palomares, *Inorg. Chim. Acta*, 2008, **361**, 684.
32 O. A. Petrov, G. V. Osipova, A. S. Semeikin and B. D. Berezin, *Russ. J. Coord. Chem.*, 2005, **31**, 894.
33 O. A. Petrov and A. V. Glazunov, *Russ. J. Coord. Chem.*, 2006, 1411.
34 J. Bisquert, G. Garcia-Belmonte, A. Pitarch and H. Bolink, *Chem. Phys. Lett.*, 2006, **422**, 184.
35 I. Mora-Seró, J. Bisquert, F. Fabregat-Santiago, G. Garcia-Belmonte, G. Zoppi, K. Durose, Y. Y. Proskuryakov, I. Oja,

A. Belaidi, T. Dittrich, R. Tena-Zaera, A. Katty, C. Lévy-Clement, V. Barrioz and S. J. C. Irvine, *Nano Lett.*, 2006, **6**, 640.
36 J. Bisquert, G. Garcia-Belmonte, J. M. Montero and H. J. Bolink, *Proc. SPIE Int. Soc. Opt. Eng.*, 2006, 6192.
37 T. C. Li, M. S. Góes, F. Fabregat-Santiago, J. Bisquert, P. R. Bueno, C. Prasittichai, J. T. Hupp and T. J. Marks, *J. Phys. Chem. C*, 2009, **113**, 18385.
38 M. Miyashita, K. Sunahara, T. Nishikawa, Y. Uemura, N. Koumura, K. Hara, A. Mori, T. Abe, E. Suzuki and S. Mori, *J. Am. Chem. Soc.*, 2008, **130**, 17874.
39 G. Boschloo and A. Hagfeldt, *Acc. Chem. Res.*, 2009, **42**, 1819.
40 Y. Cao, Y. Bai, Q. Yu, Y. Cheng, S. Liu, D. Shi, F. G. and P. Wang, *J. Phys. Chem. C*, 2009, **113**, 6290.
41 C. S. Karthikeyan, H. Wietasch and M. Thelakkat, *Adv. Mater.*, 2007, **19**, 1091.
42 S. A. Haque, E. Palomares, B. M. Cho, A. N. M. Green, N. Hirata, D. R. Klug and J. R. Durrant, *J. Am. Chem. Soc.*, 2005, **127**, 3456.
43 J. N. Clifford, E. Palomares, M. K. Nazeeruddin, M. Grätzel and J. R. Durrant, *J. Phys. Chem. C*, 2007, **111**, 6561.
44 Boschloo and Hagfeldt, *Chem. Phys. Lett.*, 2003, **370**, 381.
45 G. Sauve, M. E. Cass, G. George Coia, S. J. Doig, I. Lauermann, K. E. Pomykal and N. S. Lewis, *J. Phys. Chem. B*, 2000, **104**, 6821.
46 J. Bisquert, A. Zaban and P. Salvador, *J. Phys. Chem. B*, 2002, **106**, 8774.
47 S. Mori, M. Nagata, Y. Nakahata, K. Yasuta, R. Goto, M. Kimura and M. Taya, *J. Am. Chem. Soc.*, 2010, **132**, 4054.

